


# Impact of asymptomatic infected individuals on epidemic transmission dynamics in multiplex networks with partial coupling

Xin Hu(胡鑫), Jiaxing Chen(陈嘉兴), and Chengyi Xia(夏承遗)

**Citation:**Chin. Phys. B, 2024, 33 (**10**): 100202. DOI: 10.1088/1674-1056/ad757b
Journal homepage: http://cpb.iphy.ac.cn; http://iopscience.iop.org/cpb

**What follows is a list of articles you may be interested in**

---

## Finite-time $H_\infty$ filtering for Markov jump systems with uniform quantization

Jingjing Dong(董敬敬), Xiaofeng Ma(马晓峰), Xiaoqing Zhang(张晓庆), Jianping Zhou(周建平), and Zhen Wang(王震)
Chin. Phys. B, 2023, 32 (**11**): 110202. DOI: 10.1088/1674-1056/acedf5

## Stochastic optimal control for norovirus transmission dynamics by contaminated food and water

Anwarud Din and Yongjin Li(黎永锦)
Chin. Phys. B, 2022, 31 (**2**): 020202. DOI: 10.1088/1674-1056/ac2f32

## Evolutionary game dynamics of combining the Moran and imitation processes

Xian-Jia Wang(王先甲), Cui-Ling Gu(顾翠伶), Shao-Jie Lv(吕少杰), Ji Quan(全吉)
Chin. Phys. B, 2019, 28 (**2**): 020203. DOI: 10.1088/1674-1056/28/2/020203

## Stochastic evolutionary public goods game with first and second order costly punishments in finite populations

Ji Quan(全吉), Yu-Qing Chu(储育青), Wei Liu(刘伟), Xian-Jia Wang(王先甲), Xiu-Kang Yang(阳修康)
Chin. Phys. B, 2018, 27 (**6**): 060203. DOI: 10.1088/1674-1056/27/6/060203

## Degree distribution of random birth-and-death network with network size decline

Xiao-Jun Zhang(张晓军), Hui-Lan Yang(杨会兰)
Chin. Phys. B, 2016, 25 (**6**): 060202. DOI: 10.1088/1674-1056/25/6/060202

---

**RAPID COMMUNICATION**

# Impact of asymptomatic infected individuals on epidemic transmission dynamics in multiplex networks with partial coupling

Xin Hu(胡鑫)[1], Jiaxing Chen(陈嘉兴)[2], and Chengyi Xia(夏承遗)[3,†]

[1] *School of Control Science and Engineering, Tiangong University, Tianjin* 300387, *China*
[2] *School of Computer Science and Engineering, Tianjin University of Technology, Tianjin* 300384, *China*
[3] *School of Artificial Intelligence, Tiangong University, Tianjin* 300387, *China*

(Received 23 July 2024; revised manuscript received 29 August 2024; accepted manuscript online 30 August 2024)

The theory of network science has attracted great interest of many researchers in the realm of biomathematics and public health, and numerous valuable epidemic models have been developed. In previous studies, it is common to set up a one-to-one correspondence between the nodes of a multi-layer network, ignoring the more complex situations in reality. In the present work, we explore this situation by setting up a partially coupled model of a two-layer network and investigating the impact of asymptomatic infected individuals on epidemics. We propose a self-discovery mechanism for asymptomatic infected individuals, taking into account situations such as nucleic acid testing in the community and individuals performing self-antigen testing during the epidemic. Considering these factors together, through the microscopic Markov chain approach (MMCA) and extensive Monte Carlo (MC) numerical simulations, we find that the greater the coupling between the networks, the more information dissemination is facilitated. In order to control the epidemics, more asymptomatic infected individuals should be made aware of their infection. Massive adoption of nucleic acid testing and individual adoption of antigenic self-testing can help to contain epidemic outbreaks. Meanwhile, the epidemic threshold of the proposed model is derived, and then miscellaneous factors affecting the epidemic threshold are also discussed. Current results are conducive to devising the prevention and control policies of pandemics.

**Keywords:** asymptomatic infected individuals, multi-layer networks, partial interdependence

**PACS:** 02.50.Ga, 45.05.+x, 64.70.qd, 47.27.eb **DOI:** 10.1088/1674-1056/ad757b

## 1. Introduction

Over the past two decades, the theory of network science has made huge progress,[1,2] providing a theoretical basis for investigating the co-evolutionary characteristics of complex networks. In recent years, the study of epidemic propagation dynamics on networks has received a great deal of attention within the scientific community.[3–7] From the traditional compartmental model to multi-population models[8,9] and then to networking models,[10–12] such as the networked SIS model[13] and the SIR model,[14] the modeling of epidemics has been dominant in the field of network science. However, such models tend to assume that individuals in the same compartment are in full contact and they have the same probability of being infected by an infected agent. In reality, individuals tend to be exposed to a limited range. Therefore, it is necessary to consider the heterogeneity of individuals when modeling the spread of epidemics.[15]

During the epidemic outbreak, a large amount of disease-related information will be disseminated via the Internet, and when people realize the existence of epidemics, they may take appropriate actions to prevent themselves from being infected, such as ventilating homes and workplaces regularly. These behaviors also change the dynamic evolution of epidemics and inhibit their spread to some extent.[16–19] Funk *et al.*[20] considered the impact of awareness on epidemic dynamics and found that awareness diminishes the scale of epidemics, but does not impact the critical threshold. Differences in network topology may also affect the dynamics of infectious diseases, for example, based on the framework of multiplex networks, Granell *et al.*[21] found that there is a meta-critical point, which is defined by the structural and perceptual dynamics of the virtual layer and can influence the outbreak of epidemics. During a pandemic, society will be flooded with a large amount of information related to epidemics due to the diversity of information and transmission channels, which results in a more complex interaction between information and epidemics. Additionally, characteristics of epidemiological transmission under a variety of information have also received extensive attention from the scientific community.[22–25] By modeling awareness-epidemic transmission under mass media, Xia *et al.*[30] indicated that mass media can guide the population to adopt effective actions to avoid being infected. As a further step, Wang *et al.*[26] examined the evolution of epidemics under two opposing information and found that enabling more individuals to receive positive messages could suppress disease propagation, while negative information had the opposite effect. Huang *et al.*[27] observed that knowledge dissemination is crucial for controlling rumors and epidemic outbreaks in social networks, and that increasing the intensity of knowl-

†Corresponding author. E-mail: cyxia@tiangong.edu.cn

© 2024 Chinese Physical Society and IOP Publishing Ltd 

edge penetration into rumors can significantly increase the threshold for rumors and epidemic outbreaks. The channel of information dissemination can also greatly influence epidemic transmission dynamics.[28,29] This phenomenon was revealed in previous outbreaks of COVID-19, the specificity of the novel coronavirus led to the emergence of asymptomatically infected individuals.[31–34] Asymptomatically infected individuals do not have initial symptoms such as fever and cough, and then they may come into contact with others, including those healthy individuals without taking any protective measures.[35] The emergence of asymptomatically infected individuals can disrupt the prevention and control of epidemics, so it is necessary to consider this situation in epidemiological modeling. During the evolution of pandemics, governments and public health authorities regularly conduct virus testing on the population, and individuals also purchase corresponding self-testing medical supplies to know their own infection status. However, this scenario is neglected in many previous works, here we introduce a self-discovery mechanism in the model, where asymptomatically infected individuals can become aware of their virus infection through self-discovery measures and will transmit disease-related information to their neighbors, so as to take the impact of asymptomatically infected individuals into account.

Next, the effect of network coupling pattern between different layers of networks on transmission behaviors of information or epidemics is also explored here. On the epidemic dynamics in the multi-layer networks, the node coupling relationship between two-layer networks is often assumed to be a one-to-one correspondence,[37–39] and it is believed that once an individual receives information about the outbreak, s/he will take some preventive actions to avoid being infected; meanwhile, if an individual is infected, s/he will also disseminate the relevant information in the population.[40,41] However, the reality is often more complicated, when people are infected, there is a certain possibility that they will not spread the information in time. During the early outbreak of the COVID-19 pandemic, governments implemented stringent epidemic prevention measures. Nevertheless, some individuals, upon being infected, deliberately concealed their infection status due to the potential isolation and travel restrictions, and were unwilling to cooperate in adopting necessary protective measures. Such behaviors not only increased the risk of infection for these individuals themselves, but also posed a significant impediment to the combating efforts of the pandemics, further compounding the challenges faced by prevention and control work.[42] Given the complexity of real situations, it is necessary to fully consider the coupling relationships between nodes in a two-layer network when modeling epidemics, which helps us to more accurately understand and predict the transmission behaviors of epidemics, and thus develop more effective prevention and containment strategies.

Based on the above considerations, for the purpose of deeply investigating the influence of asymptomatic infected agents on the transmission behaviors of infectious diseases, we develop a new UAU–SEIS epidemic spreading model, where one layer stands for the disease transmission network, and the other layer stands for the information transmission network. In order to further model the role of network coupling pattern, we set the correspondence relationship of the nodes to be partial coupling, which simply means that the nodes with coupling relationship in two layers will interact with each other during the epidemic transmission process, while those without any coupling will not do so. By utilizing the microscopic Markov chain approach (MMCA), we construct the probability tree of each class of agents and establish the corresponding epidemic equations, and finally derive the expression for the epidemic threshold. Meanwhile, extensive MC numerical simulations are used to demonstrate the feasibility of MMCA, revealing the effect of asymptomatic infected individuals and partial coupling on the epidemic propagation.

The remaining sections will be organized as follows. In Section 2, the information–disease partial coupling model is described, then the probability tree is constructed and the corresponding dynamic equations are established. In Section 3, the impacts of different parameters on disease spread and information diffusion are studied through extensive numerical simulation experiments. Finally, in Section 4 we end the paper with some concluding remarks.

## 2. Model description

In this work, we develop a partially coupled two-layer network model. In order to represent the heterogeneity of the population in terms of processing information and taking action, we modify the topology and degree of the networks. In Fig. 1, the upper network layer stands for the mutual information dissemination during an outbreak, while the lower network layer denotes the population contact network where the epidemic spreads. Some of the nodes in the two layers have virtual connections between them, representing the coupling relationship between the nodes, which accompanies the disease spreading process to influence each other.

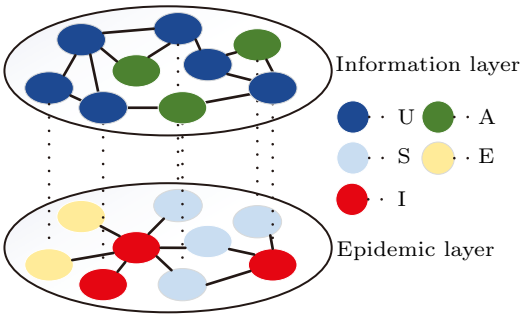



**Fig. 1.** Illustration of the coupled two-layer network and spread model. In the model under partial coupling, unaware (U) and aware (A) states exist in the information layer, while susceptible (S), asymptomatic (E) and infected (I) exist in the epidemic layer. The nodes of the two layers of the network are partially coupled to each other.

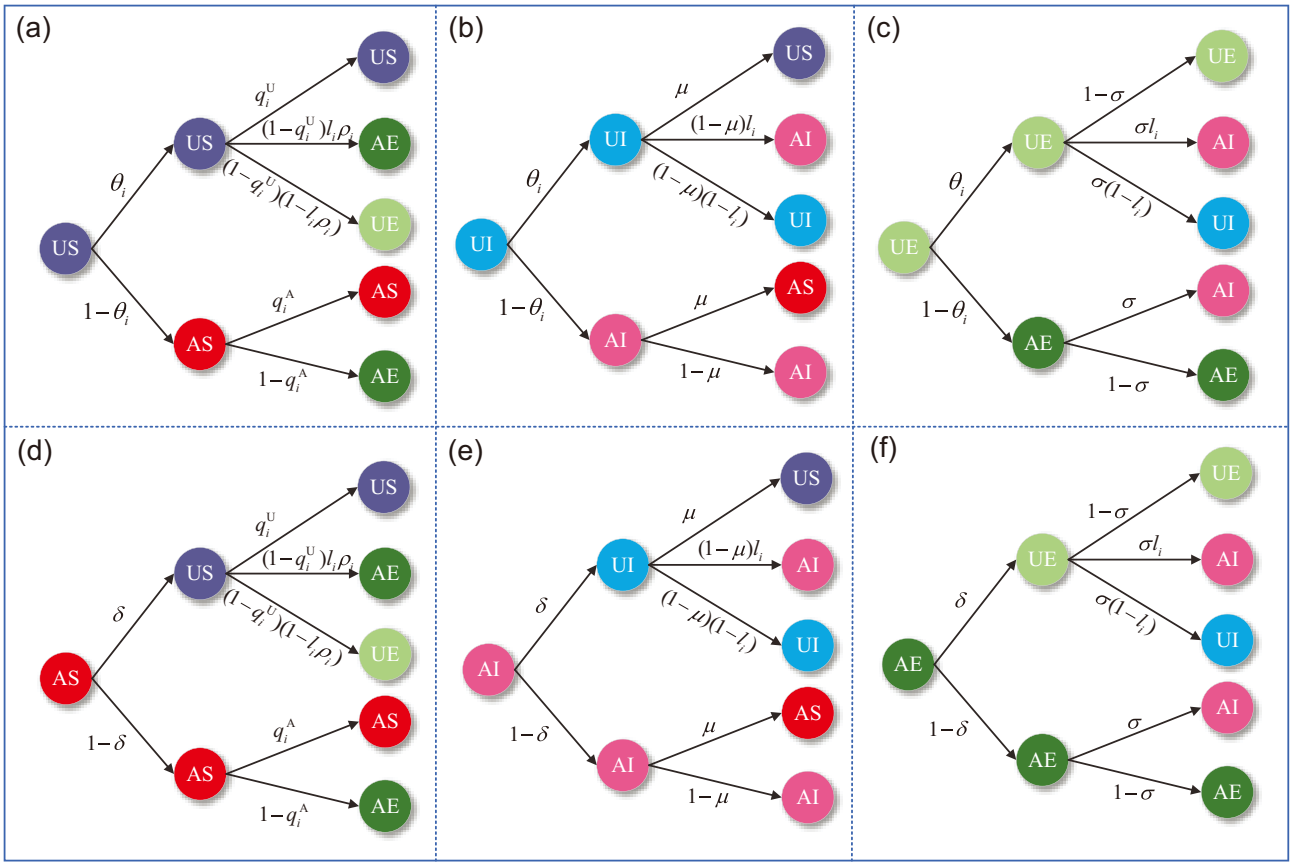



**Fig. 2.** Transformation trees for six states: (a) US state, (b) UI state, (c) UE state, (d) AS state, (e) AI state, (f) AE state. The specific expressions for $\theta_i$, $q_i^{\mathrm{U}}$ and $q_i^{\mathrm{A}}$ are described in Eq. (2)

In the first layer (information layer) of Fig. 1, the diffusion of information adopts the UAU model, where all nodes are either in the U or A state. U and A represent individuals who are unaware and aware of epidemic information, respectively. Individuals in the A-state will spread disease-related information to their adjacent nodes with probability $\lambda$. Meanwhile, an A-state individual forgets the information with probability $\delta$ and transforms to the U-state. A-state individuals will take proper preventative actions, whereas U-state individuals, lacking knowledge of epidemics, will not take corresponding preventative actions. In the second layer (epidemic layer), with the aim of investigating the influence of asymptomatic infected individuals, we utilize the SEIS model, where S represents susceptible individuals, E means asymptomatic infected individuals, and I stands for infected individuals. S individuals will be infected by E and I individuals at the propagation rate $\beta$ (in reality, the infectivity of individuals E and I is difficult to analyze quantitatively, and for simplicity we set their infectivity to be the same). In addition, E and I individuals will transform to individuals I and S at rates $\sigma$ and $\mu$, respectively. The corresponding probabilistic transformation trees are displayed in Fig. 2.

In order to construct partial coupling between the two layers of the network, the parameter $l_i$ is introduced. $l_i = 1$ if there is a virtual connection between the nodes of the two layers, whereas $l_i = 0$ indicates no connection. $l_i$ is integrated into the vector $\boldsymbol{L} = [l_1, l_2, \ldots, l_N]$. An individual who receives the information will take protective measures and his probability of infection is $\beta^{\mathrm{A}} = v_i\beta$, $\beta^{\mathrm{U}} = \beta$, $v_i$ is defined as

$$v_i = \begin{cases} \gamma\,(0 \le \gamma \le 1), & l_i = 1, \\ 1, & l_i = 0. \end{cases} \tag{1}$$

During the COVID-19 pandemic, the Chinese government arranged for medical teams to conduct regular nucleic acid testing within each community, and residents were encouraged to take nucleic acid throat swabs for self-testing.[45] To characterize this phenomenon, we introduce a mechanism for self-discovery of asymptomatic individuals. The local infection information of individual $i$ is $\rho_i^{\mathrm{local}}(t) = \sum_j^N b_{ji} P_j^{\mathrm{I}}(t)/k_i$, and the global infection information is $\rho_i^{\mathrm{global}}(t) = \sum_j^N P_j^{\mathrm{I}}(t)/N$. The probability of self-discovery by an individual in state E is $\rho_i(t) = w\rho_i^{\mathrm{local}}(t) + (1-w)\rho_i^{\mathrm{global}}(t)$, $w \in [0,1]$. In this model, an asymptomatic individual has a probability of $\rho_i$ to know her/his infection status and take some protective measures through this mechanism.

In Fig. 2, the probabilities of the states of all nodes at moment $t$ are denoted by $P_i^{\mathrm{US}}(t)$, $P_i^{\mathrm{AS}}(t)$, $P_i^{\mathrm{UE}}(t)$, $P_i^{\mathrm{AE}}(t)$, $P_i^{\mathrm{UI}}(t)$, $P_i^{\mathrm{AI}}(t)$, respectively, and $P_i^{\mathrm{US}}(t) + P_i^{\mathrm{AS}}(t) + P_i^{\mathrm{UE}}(t) + P_i^{\mathrm{AE}}(t) + P_i^{\mathrm{UI}}(t) + P_i^{\mathrm{AI}}(t) = 1$. $[a_{ij}]$ and $[b_{ij}]$ denote the adjacency matri-

ces of information layer and epidemic layer, respectively.

$$\begin{cases} \theta_i(t) = \prod_j [1 - a_{ji} P_j^{\mathrm{A}}(t)\lambda], \\ q_i^{\mathrm{U}}(t) = \prod_j [1 - b_{ji} P_j^{\mathrm{E}}(t)\beta - b_{ji} P_j^{\mathrm{I}}(t)\beta], \\ q_i^{\mathrm{A}}(t) = \prod_j [1 - b_{ji} P_j^{\mathrm{E}}(t)\beta^{\mathrm{A}} - b_{ji} P_j^{\mathrm{I}}(t)\beta^{\mathrm{A}}], \end{cases} \tag{2}$$

where $\theta_i$ denotes the probability that an unaware individual is not informed by any aware neighbor, and $q_i^{\mathrm{U}}$ and $q_i^{\mathrm{A}}$ denote the probabilities that U and A individuals are not infected, respectively. Based on the state transformation tree in Fig. 2, the epidemic dynamics equation is derived as

$$\begin{cases} P_i^{\mathrm{US}}(t+1) = P_i^{\mathrm{US}}(t)\theta_i q_i^{\mathrm{U}} + P_i^{\mathrm{AS}}(t)\delta q_i^{\mathrm{U}} + P_i^{\mathrm{AI}}(t)\delta\mu \\ \qquad + P_i^{\mathrm{UI}}(t)\theta_i\mu, \\ P_i^{\mathrm{AS}}(t+1) = P_i^{\mathrm{US}}(t)(1-\theta_i)q_i^{\mathrm{A}} + P_i^{\mathrm{AS}}(t)(1-\delta)q_i^{\mathrm{A}} \\ \qquad + P_i^{\mathrm{AI}}(t)(1-\delta)\mu + P_i^{\mathrm{UI}}(t)(1-\theta_i)\mu, \\ P_i^{\mathrm{UE}}(t+1) = P_i^{\mathrm{US}}(t)\theta_i(1-q_i^{\mathrm{U}})(1-l_i\rho_i) \\ \qquad + P_i^{\mathrm{AS}}(t)\delta(1-q_i^{\mathrm{U}})(1-l_i\rho_i) \\ \qquad + P_i^{\mathrm{UE}}(t)\theta_i(1-\sigma) + P_i^{\mathrm{AE}}(t)\delta(1-\sigma), \\ P_i^{\mathrm{AE}}(t+1) = P_i^{\mathrm{US}}(t)[\theta_i l_i\rho_i(1-q_i^{\mathrm{U}}) + (1-\theta_i)(1-q_i^{\mathrm{A}})] \\ \qquad + P_i^{\mathrm{AS}}(t)[\delta l_i\rho_i(1-q_i^{\mathrm{U}}) + (1-\delta)(1-q_i^{\mathrm{A}})] \\ \qquad + P_i^{\mathrm{UE}}(t)(1-\theta_i)(1-\sigma) \\ \qquad + P_i^{\mathrm{AE}}(t)(1-\delta)(1-\sigma), \\ P_i^{\mathrm{AI}}(t+1) = P_i^{\mathrm{UE}}(t)[\theta_i\sigma l_i + (1-\theta_i)\sigma] \\ \qquad + P_i^{\mathrm{AE}}(t)[\delta\sigma l_i + (1-\delta)\sigma] \\ \qquad + P_i^{\mathrm{AI}}(t)[\delta l_i(1-\mu) + (1-\delta)(1-\mu)] \\ \qquad + P_i^{\mathrm{UI}}(t)[\theta_i l_i(1-\mu) + (1-\theta_i)(1-\mu)], \\ P_i^{\mathrm{UI}}(t+1) = P_i^{\mathrm{UE}}(t)\theta_i\sigma(1-l_i) + P_i^{\mathrm{AE}}(t)\delta\sigma(1-l_i) \\ \qquad + P_i^{\mathrm{AI}}(t)\delta(1-\mu)(1-l_i) \\ \qquad + P_i^{\mathrm{UI}}(t)\theta_i(1-\mu)(1-l_i). \end{cases} \tag{3}$$

As $t \to \infty$, the states in Eq. (3) tend to stabilize. Thus, $P_i^{\mathrm{US}}(t+1) = P_i^{\mathrm{US}}(t) = P_i^{\mathrm{US}}$ and the same applies to the remaining states. As $\beta$ approaches the epidemic threshold, $P_i^{\mathrm{I}} = P_i^{\mathrm{UI}} + P_i^{\mathrm{AI}} = \tau_i^{\mathrm{I}} \ll 1$, $P_i^{\mathrm{E}} = P_i^{\mathrm{UE}} + P_i^{\mathrm{AE}} = \tau_i^{\mathrm{E}} \ll 1$, and then Eq. (2) can be simplifed as

$$\begin{aligned} q_i^{\mathrm{U}} &\approx 1 - \beta\sum_j b_{ji}\tau_j^{\mathrm{E}} - \beta\sum_j b_{ji}\tau_j^{\mathrm{I}}, \\ q_i^{\mathrm{A}} &\approx 1 - \beta^{\mathrm{A}}\sum_j b_{ji}\tau_j^{\mathrm{E}} - \beta^{\mathrm{A}}\sum_j b_{ji}\tau_j^{\mathrm{I}}. \end{aligned} \tag{4}$$

By substituting Eq. (4) into Eq. (3), we obtain $P_i^{\mathrm{US}} = P_i^{\mathrm{US}}\theta_i + P_i^{\mathrm{AS}}\delta$, $P_i^{\mathrm{AS}} = P_i^{\mathrm{US}}(1-\theta_i) + P_i^{\mathrm{AS}}(1-\delta)$. Substituting $P_i^{\mathrm{US}}$ and $P_i^{\mathrm{AS}}$ into Eq. (3), we get $P_i^{\mathrm{UE}} = P_i^{\mathrm{US}}(1-q_i^{\mathrm{U}})(1-l_i\rho_i) + P_i^{\mathrm{UE}}\theta_i(1-\sigma) + P_i^{\mathrm{AE}}\delta(1-\sigma)$. Similarly, $P_i^{\mathrm{AE}} = l_i\rho_i(1-q_i^{\mathrm{U}})P_i^{\mathrm{US}} + (1-q_i^{\mathrm{A}})P_i^{\mathrm{AS}} + P_i^{\mathrm{UE}}(1-\theta_i)(1-\sigma) + P_i^{\mathrm{AE}}(1-\delta)(1-\sigma)$ can be obtained. Furthermore, since $P_i^{\mathrm{I}} = P_i^{\mathrm{UI}} + P_i^{\mathrm{AI}} = \tau_i^{\mathrm{I}}$, substituting the expression from Eq. (3) into the equation yields

$$\mu\tau_i^{\mathrm{I}} = \left(1 - q_i^{\mathrm{U}}\right) P_i^{\mathrm{US}} + \left(1 - q_i^{\mathrm{A}}\right) P_i^{\mathrm{AS}}. \tag{5}$$

After Eq. (4) is inserted into Eq. (5), the following equality can be derived:

$$\left(\sum_j b_{ji}\tau_j^{\mathrm{E}} + \sum_j b_{ji}\tau_j^{\mathrm{I}}\right)\left[1 - (1-\gamma)P_i^{\mathrm{A}}\right] - \frac{\mu}{\beta}\tau_i^{\mathrm{I}} = 0. \tag{6}$$

By performing the matrix transformation, the above equation can be further changed as

$$\sum_j \left\{ \left(1 + \frac{\mu}{\sigma}\right)\left[1 - (1-\gamma)P_i^{\mathrm{A}}\right] b_{ji} - \frac{\mu}{\beta} e_{ji} \right\} \tau_j^{\mathrm{I}} = 0, \tag{7}$$

where $P_i^{\mathrm{A}}$ denotes the sum of the probabilities of the nodes whose upper states are A, $P_i^{\mathrm{A}} = P_i^{\mathrm{AI}} + P_i^{\mathrm{AS}} + P_i^{\mathrm{AE}}$, $e_{ji}$ is an element of the identity matrix, $\Lambda_{\max}(\mathbb{N})$ is defined as the maximum eigenvalue of matrix $\mathbb{N}$, $n_{ji} = \left(1 + \frac{\mu}{\sigma}\right)\left[1 - (1-\gamma)P_i^{\mathrm{A}}\right] b_{ji}$ is an element of matrix $\mathbb{N}$. The epidemic threshold is calculated as

$$\beta_{\mathrm{c}} = \frac{\mu}{\Lambda_{\max}(\mathbb{N})}. \tag{8}$$

It can be observed that the epidemic threshold is related to the propagation of information from upper layers, and that the parameters $\sigma$, $\mu$, and $\gamma$ all exert significant impacts on this threshold.

## 3. Numerical results

In this section, we conduct a number of simulations to study the factors affecting the evolutionary dynamics of the model, in particular focusing on the role of the network coupling strength and asymptomatic infections. Consider the reality that information transmission networks have more heterogeneity, while disease transmission networks have more homogeneity.[46] Therefore, for all numerical experiments, we use a BA network with $N = 1000$ nodes and $m = 3$ to construct the information dissemination layer, and an ER randomized network with $N = 1000$ nodes and $\langle k \rangle = 6$ to construct the disease propagation layer. We introduce the vector $L$ to store the coupling relationship between the two-layer networks, and describe the proportion of nodes coupled between the two-layer networks by $\phi = \frac{\sum l_i}{N} \times 100\%$. When $t = 0$, 10% nodes are initially infected and quickly become aware of the presence of epidemics.

First, we compare the values of $\rho^{\mathrm{A}}$ and $\rho^{\mathrm{EI}}$ under MMCA and MC simulations. In MC simulations, $\rho^{\mathrm{EI}} = \sum(P_i^{\mathrm{E}} + P_i^{\mathrm{I}})/N$ and $\rho^{\mathrm{A}} = \sum(P_i^{\mathrm{AI}} + P_i^{\mathrm{AS}} + P_i^{\mathrm{AE}})/N$. In MMCA, $\rho^{\mathrm{EI}} = (N_{\mathrm{E}} + N_{\mathrm{I}})/N$ and $\rho^{\mathrm{A}} = N_{\mathrm{A}}/N$, where $N_{\mathrm{E}}$ and $N_{\mathrm{I}}$ represent the numbers of nodes whose states are E and I in the lower layer, respectively, and $N_{\mathrm{A}}$ denotes the number of nodes whose state is A in the upper layer. In Fig. 3, both $\rho^{\mathrm{A}}$ and $\rho^{\mathrm{EI}}$ increase as $\beta$ increases. In panel (a), when $\beta < \beta_{\mathrm{c}}$, $\rho^{\mathrm{A}}$ remains almost constant regardless of $\beta$. However, when $\beta$ takes a larger value, $\rho^{\mathrm{A}}$ increases with the increase of coupling rate $\phi$. This indicates that an increase in coupling rate can promote the

spread of information, leading more individuals to enter the A state. In panel (b), when $\beta$ is kept constant, $\rho^{\mathrm{EI}}$ decreases with the increase of the coupling rate $\phi$. The increase of the coupling rate reduces the scale of the EI-state population and inhibits the propagation of epidemics. Furthermore, it can be observed from panels (a) and (b) that the data from MMCA and MC match well, indicating that MMCA is highly suitable for studying dynamic models. Thus, in what follows, we will proceed with the experimental results obtained by MMCA.

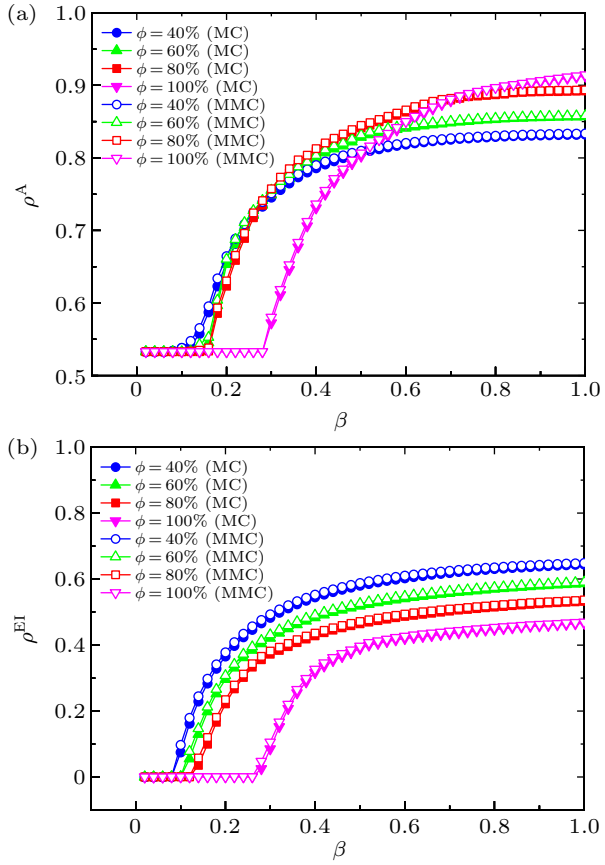



**Fig. 3.** Demonstration of MC simulations and MMCA numerical results with different parameters $\phi$. The solid pattern represents the result of MC simulation and the hollow pattern represents the result of MMCA. (a) $\rho^{\mathrm{A}}$ is plotted as a function of $\beta$; (b) $\rho^{\mathrm{EI}}$ is plotted as a function of $\beta$. The other parameter settings are $\lambda = 0.5$, $\delta = 0.6$, $\mu = 0.4$, $\gamma = 0$, $\sigma = 0.5$, and $w = 0.5$.

We then investigate the impact of different $\sigma$ on $\rho^{\mathrm{A}}$ and $\rho^{\mathrm{EI}}$ within this model. From Fig. 4(b), it can be found that when $\beta$ is constant, $\rho^{\mathrm{EI}}$ decreases as $\sigma$ increases. At $\sigma = 0.9$, $\rho^{\mathrm{EI}}$ reaches the lowest point, and $\sigma$ indicates the probability that asymptomatic infected individuals turn into infected individuals. This transition reduces the scale of the EI-state and inhibits the widespread propagation of epidemics when more asymptomatic infected individuals are more likely to turn into infected individuals. In Fig. 4(a), we observe that changes in $\sigma$ significantly affect $\rho^{\mathrm{A}}$. As $\sigma$ increases, more asymptomatic infected individuals transform into infected individuals. Once an individual is infected, he/she will immediately know the presence of the pandemic if the coupling exists, so that $\rho^{\mathrm{A}}$ increases with $\sigma$, and the increase of $\sigma$ promotes the spreading of awareness in the population.

Next, we investigate the effect of the information dissemination rate $\lambda$ on this model, from Fig. 5(a), it can be observed that larger $\lambda$ leads to larger $\rho^{\mathrm{A}}$, while in Fig. 5(b), a larger $\lambda$ leads to a smaller $\rho^{\mathrm{EI}}$. The results show that a larger $\lambda$ will lead to a wider diffusion of information in the population, and then more agents will be aware of the disease, so those in A-state will take appropriate protective actions to prevent being infected, thereby reducing the range of epidemic.

During the COVID-19 pandemic, the Chinese government regularly conducted nucleic acid testing for community residents and encouraged the purchase of appropriate medical supplies for antigenic self-testing. This allowed individuals to understand their own infection status, enabling more asymptomatic infected ones to be aware of their infection status and take appropriate measures. In our model, we describe this phenomenon by introducing a self-testing mechanism. During the numerical experiments, we consider the impact of varying awareness factors $w$ on the model. As shown in Fig. 6, when $\beta$ is constant, $\rho^{\mathrm{A}}$ increases with the increase in $w$, making it easier for asymptomatic infected individuals to realize that they are infected and thus avoid infecting other susceptible individuals. Therefore, $\rho^{\mathrm{EI}}$ will decrease as $w$ increases.

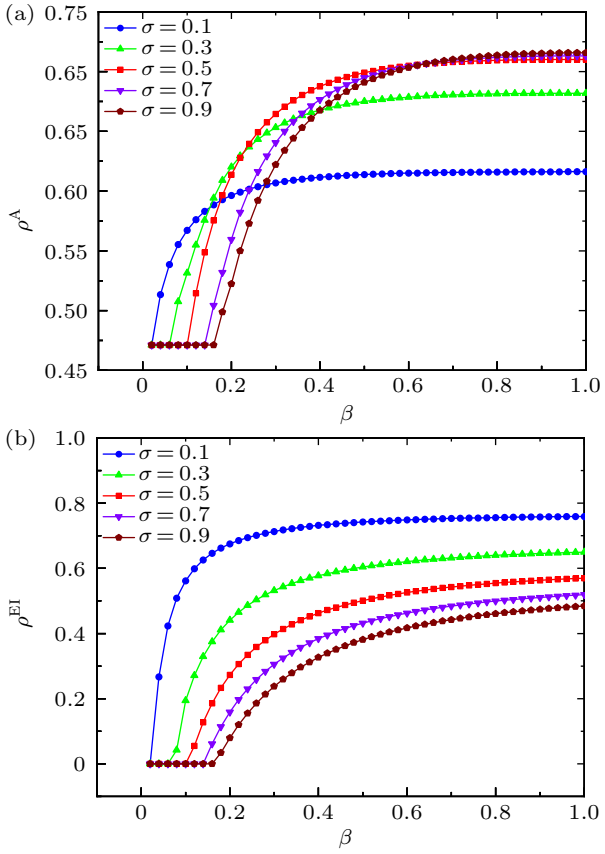



**Fig. 4.** Demonstration of MMCA numerical results with different parameters $\sigma$. (a) $\rho^{\mathrm{A}}$ is plotted as a function of $\beta$; (b) $\rho^{\mathrm{EI}}$ is plotted as a function of $\beta$. Here $\lambda = 0.2$, $\delta = 0.4$, $\mu = 0.4$, $\gamma = 0$, $w = 0.5$, and $\phi = 80\%$.

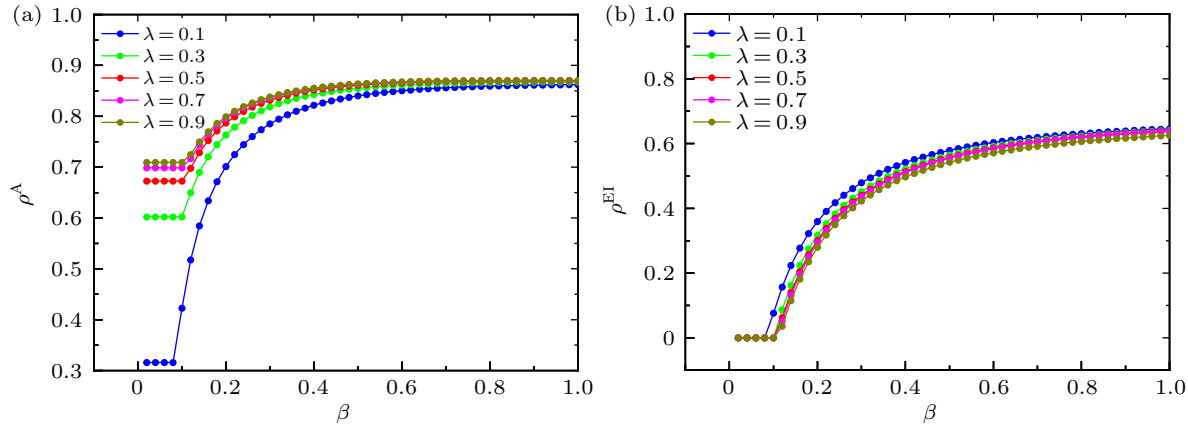



**Fig. 5.** Demonstration of MMCA numerical results with different parameters $\lambda$. (a) $\rho^{A}$ is plotted as a function of $\beta$; (b) $\rho^{EI}$ is plotted as a function of $\beta$. The other parameter settings are $\delta = 0.5$, $\mu = 0.5$, $\gamma = 0$, $\sigma = 0.6$, $w = 0.5$, and $\phi = 80\%$.

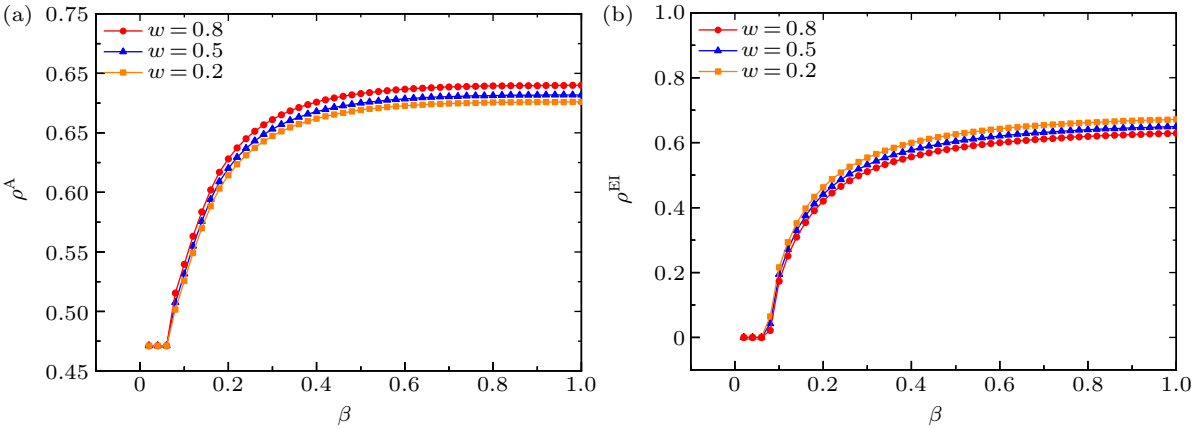



**Fig. 6.** Demonstration of MMCA numerical results with different parameters $w$. (a) $\rho^{A}$ is plotted as a function of $\beta$; (b) $\rho^{EI}$ is plotted as a function of $\beta$. The other parameter settings are $\lambda = 0.3$, $\delta = 0.4$, $\mu = 0.5$, $\gamma = 0.5$, $\sigma = 0.4$, and $\phi = 90\%$.

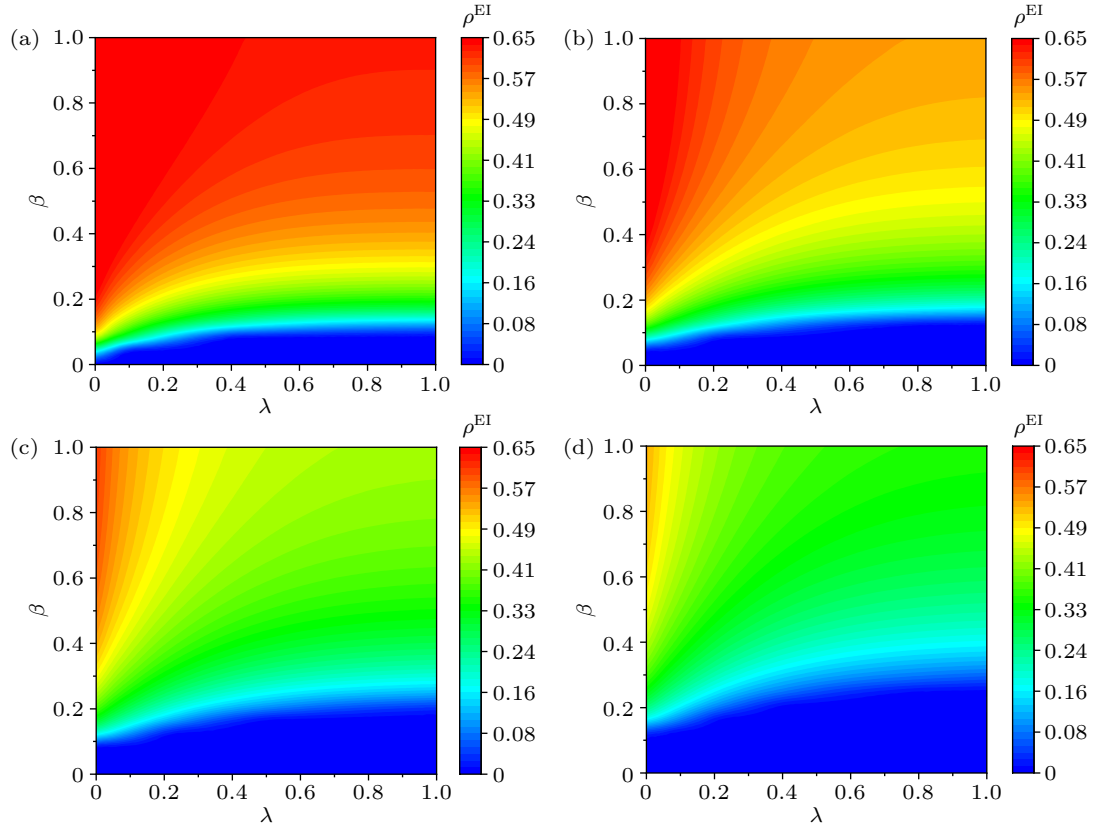



**Fig. 7.** The full phase diagrams of $\rho^{EI}$ as a function of $\lambda$ and $\beta$. The correspondence rate $\phi$ is set as follows: (a) $\phi = 40\%$, (b) $\phi = 60\%$, (c) $\phi = 80\%$, (d) $\phi = 100\%$. Here $\delta = 0.5$, $\mu = 0.3$, $\gamma = 0$, $\sigma = 0.5$, and $w = 0.5$.

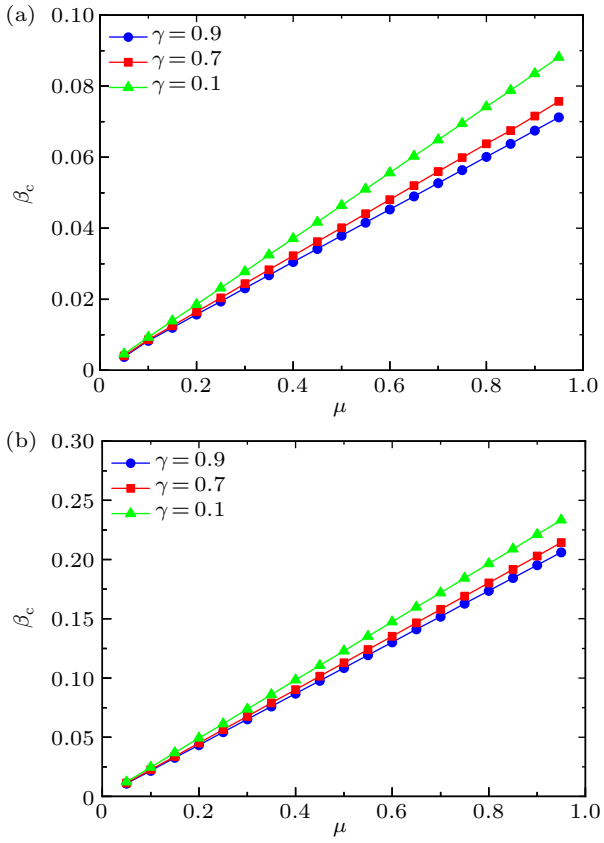



**Fig. 8.** The $\beta_c$ as a functions of $\mu$ under different $\gamma$ and $\phi$. The correspondence rate $\phi$ is set as follows: (a) $\phi = 100\%$, (b) $\phi = 50\%$. Here $\lambda = 0.3$, $\delta = 0.4$, $w = 0.5$, and $\sigma = 0.4$.

In order to further investigate the impact of coupling rate on the model, then we plot the full phase diagrams of $\rho^{\mathrm{EI}}$ at different coupling rates. From Fig. 7, it can be found that $\rho^{\mathrm{EI}}$ decreases with decreasing $\beta$ when $\lambda$ is kept constant, and $\rho^{\mathrm{EI}}$ decreases with increasing $\lambda$ when $\beta$ is kept constant. It is indicated that enhancing the dissemination of information related to epidemic can considerably diminish the massive infection of the population when controlling the epidemic. By comparing panels (a)–(d), it is found that as the coupling rate $\phi$ gradually increases, $\rho^{\mathrm{EI}}$ decreases, which shows that the coupling rate is crucial for controlling the epidemic. In this model, the increase of the coupling rate will make more infected people realize the existence of epidemic, so that they can take protective measures and participate in the diffusion of information related to epidemic.

Finally, we explore the influence of varying attenuation components $\gamma$ on the epidemic threshold. The attenuation factor $\gamma$ characterizes the extent to which individuals take strong or weak preventive measures. In Fig. 8, it is clearly shown that as the value of $\gamma$ decreases, the threshold $\beta_c$ gradually increases. This indicates that when each individual is able to take effective preventive measures, it becomes difficult for infectious diseases to break out in the population. Furthermore, as the recovery rate $\mu$ increases gradually, $\beta_c$ is increasing. This suggests that improving medical resources during a pandemic can effectively prevent the outbreak of an epidemic, as better medical resources allow individuals to receive treatment earlier. By comparing panels (a) and (b), it is evident that at the higher coupling rate, the larger threshold $\beta_c$ is obtained. This demonstrates that enhancing the coupling rate can raise the epidemic threshold, thus confirming the experimental results in Fig. 7.

## 4. Conclusion

In this work, we establish a novel epidemic model on the framework of partially coupled multiplex networks, and then investigate the effect of asymptomatic infected individuals on the epidemic transmission process. The proposed model consists of a two-layer network, where one layer stands for the information diffusion layer and the other one represents the disease propagation layer, and the nodes are partially coupled with each other between the two layers. For the purpose of studying the effect of individual antigen self-testing during pandemics on the epidemic behaviors, we construct the self-discovery mechanism of asymptomatic infected individuals, who can have a certain probability of knowing their infection automatically. By constructing the dynamic equations of the model and conducting theoretical derivations, we derive the corresponding expression for the epidemic threshold. Finally, through extensive MC simulations and data analysis, we find that a higher coupling rate leads to more infected individuals participating in the dissemination of disease-related information and inhibits the propagation of epidemics. For asymptomatically infected individuals, earlier detection of their infection can lead to the adoption of protective measures in time, which can help to avoid infecting more susceptible individuals. The government and public health departments can optimize the community nucleic acid testing programs, and rationalize the allocation of anti-epidemic resources and individuals can also adopt antigenic self-testing. Current work indicates that increasing the rate of information dissemination can effectively reduce the scale of epidemic, and enhancing the conversion rate of asymptomatic carriers can raise the epidemic threshold. Therefore, we recommend that government agencies strengthen the promotion of epidemic information during the pandemics and implement community testing measures to detect asymptomatic carriers early and isolate them.

## Acknowledgment

Project supported by the National Natural Science Foundation of China (Grant No. 62173247).

## References

[1] Boccaletti S, Latora V, Moreno Y, Chavez M and Hwang D U 2006 *Phys. Rep.* **424** 175
[2] Wang Z, Wang L, Szolnoki A and Perc M 2015 *Eur. Phys. J. B* **88** 124
[3] Salehi M, Sharma R, Marzolla M, Magnani M, Siyari P and Montesi D 2015 *IEEE Trans. Netw. Sci. Eng.* **2** 65

[4] Ma X, Cui Y P, Yan X L, Ni S J and Shen S F 2019 *Chin. Phys. B* **28** 128901
[5] Nian F Z and Yang Y 2024 *Chin. Phys. B* **33** 058705
[6] Zhu Y, Shen R, Dong H and Wang W 2024 *Chin. Phys. B* **33** 058301
[7] Juher D, Rojas D and Saldaa J 2023 *Phys. Nonlinear Phenom.* **448** 133714
[8] Hanski I 1998 *Nature* **396** 41
[9] Keeling M J and Gilligan C A 2000 *Nature* **407** 903
[10] Pastor-Satorras R and Vespignani A 2001 *Phys. Rev. E* **63** 066117
[11] Newman M E 2002 *Phys. Rev. E* **66** 016128
[12] Ward J A and Grindrod P 2014 *Phys. Nonlinear Phenom.* **282** 27
[13] Gray A, Greenhalgh D, Hu L, Mao X and Pan J 2011 *SIAM J. Appl. Math.* **71** 876
[14] McCluskey C C 2010 *Nonlinear Anal. Real World Appl.* **11** 55
[15] Chen J, Feng M, Zhao D, Xia C and Wang Z 2023 *IEEE Trans. Syst. Man Cybern. Syst.* **53** 7415
[16] Funk S, Gilad E and Jansen V A 2010 *J. Theor. Biol.* **264** 501
[17] Granell C, Gmez S and Arenas A 2014 *Phys. Rev. E* **90** 012808
[18] Xu Y, Wang J, Xia C and Wang Z 2023 *Sci. China Inf. Sci.* **66** 222208
[19] Wu Y, Wang X and Jiang G P 2024 *Chin. Phys. B* **33** 040205
[20] Funk S, Gilad E, Watkins C and Jansen V A A 2009 *Proc. Natl. Acad. Sci. USA* **106** 6872
[21] Granell C, Gmez S and Arenas A 2013 *Phys. Rev. Lett.* **111** 128701
[22] Guo Q, Jiang X, Lei Y, Li M, Ma Y and Zheng Z 2015 *Phys. Rev. E* **91** 012822
[23] Zheng C, Xia C, Guo Q and Dehmer M 2018 *J. Parallel Distrib. Comput.* **115** 20
[24] Zhu Y, Xia C and Chen Z 2023 *IEEE Trans. Autom. Control* **68** 5798
[25] Jin Y L, Han Q Y, Guo R Z, Gao Y and Shen L Q 2023 *Chin. Phys. B* **32** 100507
[26] Xia C, Wang Z, Zheng C, Guo Q and Shi Y 2019 *Inf. Sci.* **471** 185
[27] Wang Z, Xia C, Chen Z and Chen G 2021 *IEEE Trans. Cybern.* **51** 1454
[28] Huang H, Chen Y and Ma Y 2021 *Appl. Math. Comput.* **388** 125536
[29] Sharevski F, Huff A, Jachim P and Pieroni E 2022 *Int. J. Inf. Manag. Data Insights* **2** 100059
[30] Tan E Y, Albarazi D, Saw Y E, Buvanaswari P, Doshi K and Liu J C 2021 *J. Migr. Health* **4** 100069
[31] Li L, Zhang Q, Wang X, Zhang J, Wang T, Gao T L, Duan W, Tsoi K K and Wang F Y 2020 *IEEE Trans. Comput. Soc. Syst.* **7** 556
[32] Laing A G, Lorenc A, Del Molino Del Barrio I, Das A, Fish M, Monin L, Muoz-Ruiz M, McKenzie D R, Hayday T S and Francos-Quijorna I 2020 *Nat. Med.* **26** 1623
[33] Overton C E, Stage H B, Ahmad S, Curran-Sebastian J, Dark P, Das R, Fearon E, Felton T, Fyles M and Gent N 2020 *Infect. Dis. Model.* **5** 409
[34] Yu X and Yang R 2020 *Influenza Other Respir. Viruses* **14** 474
[35] Wang H, Ma C, Chen H S and Zhang H F 2021 *Appl. Math. Comput.* **400** 126084
[36] Saad-Roy C M, Wingreen N S, Levin S A and Grenfell B T 2020 *Proc. Natl. Acad. Sci. USA* **117** 11541
[37] Huo L and Wu B 2024 *Chin. Phys. B* **33** 038702
[38] Sun Q, Wang Z, Zhao D, Xia C and Perc M 2022 *Chaos Solitons Fractals* **164** 112734
[39] Huang S, Chen J, Li M Y, Xu Y H and Hu M B 2024 *Chin. Phys. B* **33** 030205
[40] Sahneh F D, Chowdhury F N and Scoglio C M 2012 *Sci. Rep.* **2** 632
[41] Verelst F, Willem L and Beutels P 2016 *J. R. Soc. Interface* **13** 20160820
[42] Shi Y, Jiang H L, Yang M X, Dong L J, Chen Y, Zhou Y B and Jiang Q W 2021 *Infect. Dis. Poverty* **10** 58
[43] Njozing B N, Edin K E, Sebastin M S and Hurtig A K 2011 *BMC Int. Health Hum. Rights* **11** 1
[44] Kruger W, Lebesa N, Lephalo K, Mahlangu D, Mkhosana M, Molise M, Segopa P and Joubert G 2020 *Afr. J. AIDS Res.* **19** 156
[45] Liu W, Yue X G and Tchounwou P B 2020 *Int. J. Environ. Res. Public Health* **17** 2304
[46] Liu Z, Lai Y C and Ye N 2003 *Phys. Rev. E* **67** 031911